4 Injection Systems

4.1 Introduction

The injection system must provide the electrons and positrons for the beams of the two linacs. The low-energy beams must be accelerated to 5 GeV before being first injected into damping rings to reduce their emittances (chapter 5), after which they are sent through bunch compressors (chapter 6) before injection into the main linacs.

The electron linac will be supplied with beam from three separate injectors, depending on the mode of operation:

- a polarised electron gun for the collider;

- a laser driven RF gun for the collider;

- a laser driven RF gun for the free electron laser (FEL, section 9.3).

Although the polarised injector is intended as the primary source for the collider, the RF gun can be used as a commissioning gun and as a backup to the polarised source: this is particularly prudent given the additional complexity and R&D required for the polarised gun, whereas the RF gun (unpolarised) source is essentially a copy of the TTF gun. The use of two different RF guns for the collider and FEL is a result of the different beam characteristics for optimal performance of the two modes of operation.

The three electron sources share a common superconducting electron injection linac (based on the main linac design, see chapter 3) for acceleration to 5 GeV. For convenience, the beams from the three sources are injected into the 5 GeV linac at a common nominal energy of 500 MeV.

The positron source is based on the concept of high-energy photon conversion into e^+e^- pairs in a thin rotating target. This scheme has the advantage of a low heat load on the target and a relatively high capture efficiency. The photons are generated by sending the high energy electron beam (150–250 GeV) through a long planar undulator magnet placed upstream of the interaction point. The generated positron beam has a large longitudinal and transverse emittance, and solenoids are required for focusing; this precludes the use of a superconducting accelerator, and normal-conducting copper cavities must be used. The copper cavities can also withstand the relatively high particle losses expected in the region. An adiabatic matching device adapts the phase space of the beam emerging from the target to the acceptance of the solenoid focused linac. After acceleration to 250 MeV, the positron beam is further accelerated in a

superconducting linac (the positron injection linac) to an energy of 5 GeV. Replacing the planar undulator magnet by a helical undulator will open up the possibility of generating polarised positron beams.

It is inconvenient to use the high energy electron beam for positron production during the commissioning and initial 'tuning' phase of the positron linac. Therefore, for tuning purposes it is planned to construct an *auxiliary* low intensity positron source, based on a 500 MeV electron beam striking the same target. The electron beam is generated from a source of the same type used for the main electron injector. This source (without the conversion target) could also be used in an alternative commissioning scheme, where the positron systems would be operated with electrons (note that switching magnet polarities in the various sub-systems is also required for the e^-e^- and $\gamma\gamma$ collider modes of operation).

4.2   The Electron Injectors

Figure 4.2.1 shows the overall concept of the electron injector complex foreseen for TESLA. The three electron sources can be installed in tunnels at different depths below ground level, one above the other. Alternatively, the three injectors can be placed at the same depth with the main axis shaft leading to one injector and with tunnels connecting the injectors together. A pulsed bending magnet will be used to select which injector provides beam to the 5 GeV injector linac for a given pulse. Two of the electron injectors will require an additional dipole. Since beam quality is most critical for the FEL, the FEL injector will be placed on the same axis as the linac. The injectors will be separated from the injector linac tunnel by an access shaft which will allow equipment installation for the linac. Access for installation and maintenance of the injectors will be via the common shaft at the gun end.

All klystrons will be housed together in a suitable location outside of the tunnel. Because of the critical nature of the injector operation, several additional back-up klystrons will also be installed, allowing fast switching in the event of a failure.

4.2.1   Unpolarised injector

4.2.1.1   RF gun and booster cavity

The advances in the field of laser driven RF guns make them attractive candidates for the unpolarised electron source. The TTF photoinjector gun [1] serves as a basis for the TESLA gun, and consists of a normal conducting 1-1/2 cell L-band standing wave cavity operated in TM_{010} mode. Solenoidal focusing is used to provide emittance compensation against the detrimental effects of space charge [2]. A high cathode gradient (35 MV/m) is needed to ensure good beam quality; this gradient is achieved by powering the gun with a 4.5 MW klystron, resulting in an output energy of approximately 4 MeV.

The TTF gun uses a Cs_2Te photocathode, which has a high quantum efficiency ($> 1\%$) and long life-time (> 1000 h) [3]. The life-time is critically dependent on
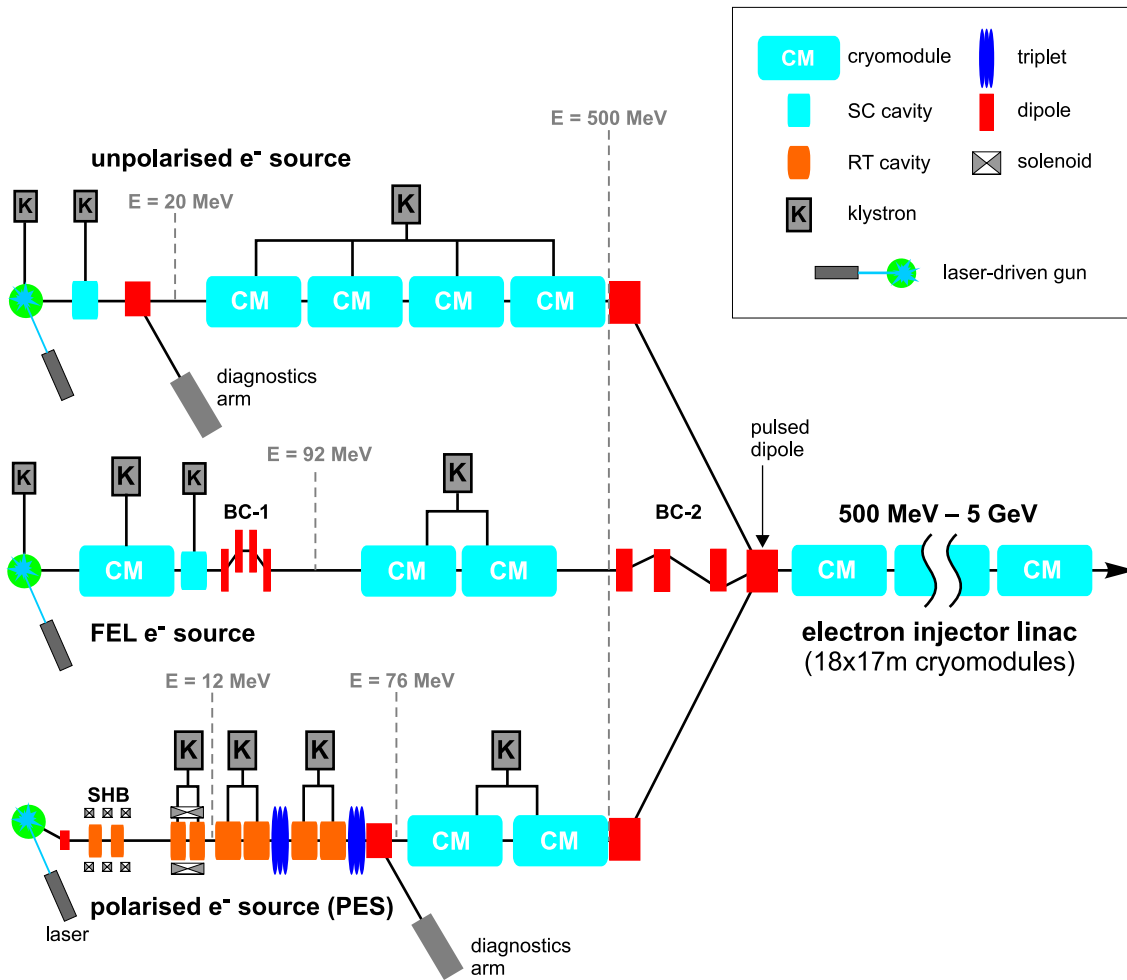
Figure 4.2.1: *Schematic of the electron injector complex (see relevant sections for details). Note that not all components are shown.*

the vacuum quality inside the gun, and so a photocathode preparation and 'load-lock' system is necessary to maintain ultra-high vacuum conditions while changing cathodes. Such systems have already been developed for TTF [4]. The laser required to provide the beam time structure for TESLA has also been developed for the TTF linac and is described below.

Similar to the TTF scheme, the electrons leaving the gun are are 'boosted' to an energy of 20 MeV by a single superconducting (SC) 9-cell cavity. The booster cavity needs a dedicated klystron of relatively low power (< 200 kW). A low level RF control system using digital signal processors has been developed at TTF to maintain the phase and amplitude constant during the 1 ms pulse. The gun-booster assembly will be separated from the rest of the injector by a short dipole spectrometer which will allow the quality of the 20 MeV beam to be checked when necessary.

The TTF gun provides symmetric normalised horizontal and vertical emittances of

Parameter	TESLA 500	TESLA 800
wavelength	<270 nm	
Train rep. rate	5 Hz	3 Hz
Pulse Train Structure:		
Pulse train length	950 μs	860 μs
No. of pulses per train	2820	4886
Pulse spacing	337 ns	176 ns
Pulse energy	3 μJ	2 μJ
Pulse length	10 ps (sigma)	
Spot radius on cathode	3 mm (flat top)	
Synchronization	to reference RF signal	
Phase stability	< 1 ps (rms)	
Energy stability	< 5 % (rms)	
Control	fully remote	
Maintenance downtime	<1 %	

Table 4.2.1: *Basic specifications of the laser system for the unpolarised electron source. The differences in the pulse train structure for both TESLA-500 and TESLA-800 are shown.*

typically 10 mm mrad at 4 nC; this exceeds the required value for the vertical emittance at the interaction point by almost two orders of magnitude, and thus a damping ring is required. A potential alternative 'flat beam' gun is currently under study, which might provide asymmetric beams with sufficiently low vertical emittance to remove the need for the electron damping ring, or at least simplify it. Some details can be found in [5].

4.2.1.2   Laser for the unpolarised RF gun

The laser system for the unpolarised source is based on the photoinjector laser system used at the TTF. A description of the laser and a discussion of the experience with its operation can be found in [18]. Basic specifications of the TESLA laser system are listed in table 4.2.1.

An important feature of the laser system is the generation of a stable $\sim$1 ms long train of UV laser pulses synchronized with the RF of the accelerator. Currently available lasers can produce the required bunch charge when used in combination with a Cs_2Te-photocathode with a quantum efficiency of $\sim$1%. At TTF, such cathodes have been operated for several thousands of hours with a stable quantum efficiency of 0.5 %. With this number, a single UV laser pulse energy in the μJ-range has to be achieved, which the TTF laser can already supply.

The laser is based on flashlamp pumped Nd:YLF rods lasing at 1047 nm. This material has a long fluorescence lifetime, high induced emission cross-section, and very small thermal lensing — all of which are favorable for long pulse trains. A mode-
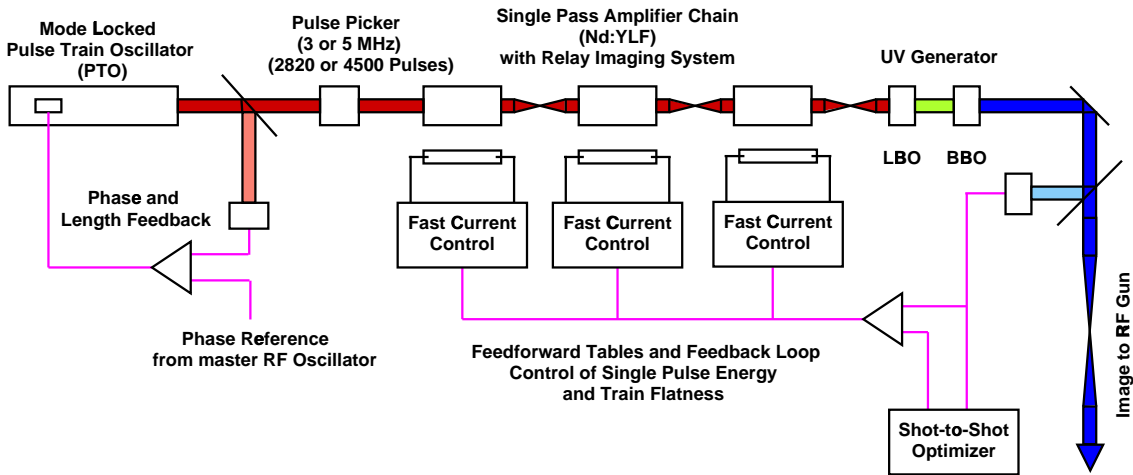
Figure 4.2.2: *Schematic of the laser system for the unpolarised RF gun source.*

locked pulse train oscillator (see figure 4.2.2) synchronized with the reference RF signal generates a pulse train with a suitable multiple of the required pulse train frequency (e.g. 30 MHz). A Pockels-cell based pulse picker running at 3 MHz for TESLA-500 (5 MHz for TESLA-800) forms the required pulse train. At TTF, a Pockels-cell is being operated at 2.25 MHz, and 9 MHz is in preparation. The train is amplified by a single pass amplifier chain to 150 μJ per pulse, corresponding to an average laser beam power of 2 W. The UV wavelength (262 nm) is generated with two non-linear crystals (e.g. LBO and BBO). The conversion efficiency is in the range of 10 %, and an energy stability in the UV of ±5 % (rms) is achievable. The bandwidth of Nd:YLF is sufficiently large to obtain a pulse length of 10 ps. The laser system will be fully remote controlled. At TTF, the photoinjector laser system has achieved an availability close to 99 %.

4.2.1.3   The 500 MeV pre-accelerator linac

Acceleration to 500 MeV takes place in four TTF type accelerator modules, each containing eight 9-cell cavities. The modules are driven by a single 10 MW klystron operating well below its maximum power capacity. The use of four modules implies a very moderate accelerating gradient for the pre-accelerator ($\sim$ 15 MV/m) in comparison with the main linac[1].

4.2.2   Polarised electron injector

A specific study for a TESLA polarised electron gun has not yet been carried out. The design for TESLA gun is therefore based on the parameters of the gun proposed for

---

[1]It should be noted that the choice of using four 12 m long TTF-like modules in the injection system design is not crucial, and they could easily be replaced by three 17 m modules of the standard main linac type (section 3.3)

Parameters	units	TESLA	NLC
Gun bunch charge	nC	4.5	
Bunch FWHM at gun	ns	2	0.7
Peak current	A	2.25	6.4
Cathode bias voltage	kV	-120	
Edge emittance	mm·mrad	8	
Beam radius	mm	12	
Envelope angle	mrad	10	
Bunch # per pulse		2820	90
Bunch spacing	ns	337	1.4
Pulse length	μs	950	0.13
Repetition rate	Hz	5	120

Table 4.2.2: *Specifications for TESLA and NLC polarised electron source.*

the NLC project [8], which is specified to deliver approximately the same bunch charge (table 4.2.2).

The TESLA time structure is quite different from the NLC: a specifically developed laser is required for the longer macropulse. We have assumed an initial bunch length of 2 ns rather than 700 ps for NLC. The transverse emittance is assumed to be the same which is a conservative assumption due to the smaller TESLA peak current. The longer initial bunch excludes the use of the NLC scheme for the prebunching section: therefore prebunching cavities of a lower frequency are chosen which follow the design for the S-Band collider Test Facility injector, described in [20].

4.2.2.1   Polarised electron gun

Polarised electrons are produced by illuminating a GaAs cathode with circularly polarised laser light. GaAs photocathodes require ultra-high vacuum conditions ($< 10^{-11}$ mbar) which are not compatible with high gradient RF gun operation. Although work is in progress to develop a polarised RF gun, we will consider here only a polarised gun based on the technology developed for SLC [7] and under further development for NLC [8].

The TESLA gun is operated with 1 ms long high voltage pulses of 120 kV with a repetition rate of 5 Hz. The accelerating field is 1.8 MV/m, the perveance 0.3 μA/V$^{3/2}$. The strained-lattice GaAs cathode has a large surface area of 3 cm^2, and is illuminated by circularly polarised laser light of 840 nm wavelength.

The gun is equipped with a load-lock system which allows the cathode to be retracted while maintaining the ultra-high vacuum in the gun. To simplify the load-lock system, an inverted insulator geometry is foreseen [9].

To avoid damage of the cathode by ion bombardment, the dark current must be kept as low as possible; this requires low fields at the electrodes, and a careful processing of the gun. The SLC gun operates at 120 kV with a dark current of less than 50 nA, and the highest field on the electrodes is 7 MV/m [7]. The TESLA gun will be operated at

a gradient of only $1.8\,\mathrm{MV/m}$ (as discussed for the NLC gun) which should significantly reduce the dark current.

The low accelerating gradient limits the extractable beam current due to space charge effects. The current can be estimated using the Child-Langmuir law: a typical perveance of $0.3\,\mu\mathrm{A/V}^{3/2}$ yields a current of $12.5\,\mathrm{A}$ at $120\,\mathrm{kV}$.

A more severe limitation specific to GaAs-type cathodes is the so-called 'cathode charge limit', which is in fact a current density limit [10]. The limitation is typical for semiconductor cathodes with a negative electron affinity surface. In order to achieve a high electron extraction probability, an alkali coating is applied to the surface of the GaAs crystal[1]. This limit can be estimated using SLC data [12]: the SLC gun has a current density limit of $3.3\,\mathrm{A/cm}^2$. For the TESLA cathode with a surface area of $3\,\mathrm{cm}^2$, the extractable current is limited to $10\,\mathrm{A}$ which is below the previous limit set by the perveance.

With a bunch charge of $3.2\,\mathrm{nC}$ ($2.2\,\mathrm{nC}$ for TESLA 800), a bunch length of at least $320\,\mathrm{ps}$ is required to keep the peak current below the $10\,\mathrm{A}$ limit. A bunch length of $2\,\mathrm{ns}$ has been chosen to ease the design of the laser system.

For multibunch operation, an additional effect related to the cathode charge limit becomes important. The effect causes a considerable reduction in bunch charge for pulse trains with very small bunch spacing. Experiments at the SLC have shown that the recovery time of the cathode is between of 10 to $100\,\mathrm{ns}$, depending on the cathode thickness [7]. Fortunately, the bunch spacing at TESLA is large, $337\,\mathrm{ns}$ ($189\,\mathrm{ns}$ for TESLA 800), so that the cathode can easily recover between bunches.

A high degree of polarisation is required to fully explore the physics potential of the collider. At SLC, $80\,\%$ polarisation with a strained lattice GaAs cathode has been achieved, but with a quantum efficiency of only 0.1% [13]. The quantum efficiency determines the required laser power, and hence has a direct impact on the design of the laser system. Maintaining good quantum efficiency requires a careful control of the vacuum, which should be kept below $10^{\cdot -11}\,\mathrm{mbar}$ at all times. Regular coating of the cathode by cesium may also be necessary.

In the NLC proposal, the gun is placed at a $20°$ angle to the injector axis, an arrangement that we will also adopt. The arrangement has several advantages: shielding of the cathode from reverse dark current produced by the downstream cavities; allowing installation of a second gun (a backup PES or a thermionic grid gun); and allowing space for a polarimeter.

4.2.2.2 Polarised gun laser

Most polarised electron sources use Ti:Sapphire lasers with a wavelength around $800\,\mathrm{nm}$. The lasers have a sufficient bandwidth to tune the wavelength to optimize the electron beam polarisation.

TESLA requires a long laser pulse train of $1\,\mathrm{ms}$, consisting of several thousand pulses with an energy of $\sim5\,\mu\mathrm{J}$ per pulse. A laser system delivering such a pulse structure is commercially not available and requires considerable R & D. Presently, a

---

[1]A discussion of the theory of the effect can be found in [11].

Parameter	TESLA 500	TESLA 800
Wavelength	780 to 850 nm	
	tunable to < 10 nm	
Train rep. rate	5 Hz	3 Hz
Polarisation	circular	
	switchable	
Pulse Train Structure:		
Pulse train length	950 μs	850 μs
No. of pulses per train	2820	4500
Pulse spacing	337 ns	189 ns
Pulse energy	4.6 μJ	3.2 μJ
Pulse length	700 ps to 2 ns (sigma)	
Spot radius on cathode	10 mm (flat top)	
Synchronization	to reference RF signal	
Phase stability	< 200 ps (rms)	
Energy stability	$< 5\,\%$ (rms)	
Control	fully remote	
Maintenance down time	$<1\,\%$	

Table 4.2.3: *Basic specification of the laser system for the polarised electron source. The differences in the pulse train structure for TESLA-500 and TESLA-800 are shown.*

laser system for the photoinjector test stand at DESY-Zeuthen is under development [14], which will serve as a test bed for the polarised gun laser. The basic specification of the laser system is given in table 4.2.3.

There are several disadvantages of the choice of Ti:Sapphire with respect to the long TESLA pulse train. The life-time of the upper laser level is only $3.2\,\mu$s, and hence the pump energy can only be stored for a short fraction of the pulse train. In addition, flashlamp pumping is not efficient. Consequently it is necessary to provide a complete laser system to pump the Ti:Sapphire for every bunch of the train. The pump lasers will be very similar to the laser for the unpolarised source: a mode-locked Nd:YLF laser with the required pulse train structure will be doubled in frequency to produce the green wavelength necessary for pumping.

Thermal properties — like thermal lensing — are also not favorable for Ti:Sapphire. Its strong thermal lensing will lead to a variation of the focusing of the laser beam during the pulse train resulting in an undesired non-uniformity, which must be compensated.

Other laser materials which are tunable in the required wavelength range are Cr:LiCAF and Cr:LiSAF. They have the advantage of low thermal lensing and the possibility of pumping by flashlamps or laser diodes [15]. Mode locked Cr:LiSAF lasers and regenerative amplifiers have been successfully built [16], but high quality materials are still difficult to obtain. A laser based on Cr:LiSAF/Cr:LiCAF is discussed in the

proposal for the TTF laser system [17].

A third possibility under study is based on an energy upgraded version of the laser proposed for the unpolarised source (section 4.2.1.2): the second and third harmonic of the fundamental laser wavelength (1047 nm) is converted to 840 nm by optical parametric amplification.

4.2.2.3   Polarised electron pre-accelerator linac

The low energy electrons produced by the polarised source cannot be directly injected into superconducting cavities because solenoids are required for transverse focusing. The electrons are first accelerated in normal-conducting copper cavities until the divergence of the beam is small enough that solenoid focusing is no longer required. Because the gun produces a long initial bunch length (2 ns), a prebunching and bunching system is also required.

The injector linac for the polarised electron beam will include:

- a prebunching and bunching section;

- an accelerating section;

- a matching and analysing section; and

- two accelerator modules to reach 500 MeV.

The injection linac is described in more detail in [19].

The prebunching section

We use two sub-harmonic prebunching cavities (SHB) working at 1/12 and 1/3 of the injector linac frequency, i.e. 108 and 433 MHz respectively. Simulations with the PARMELA code have been performed, assuming an initially uniform longitudinal distribution[1] of charges with a length of 2 ns. The optimum modulating peak voltages of the 108 MHz and 433 MHz cavities were found to be 40 kV and 44 kV respectively. The bunches are compressed to ∼190 ps rms at the entrance to the second cavity, and to ∼50 ps rms at the buncher entrance.

The power requirements have been scaled from the data for the buncher cavity used in the low charge TTF injector [21]; this cavity operates at 217 MHz and can handle a 1 ms long RF macropulse. We expect a shunt impedance R_s=4.4 MΩ for the 108 MHz cavity and R_s=8.8 MΩ for the 433 MHz cavity. The required peak power is then 360 W and 220 W respectively.

The bunching section

The cavities for the bunching section have to withstand 1 ms long RF pulses and a 0.5% duty cycle, which implies severe thermal loads. Requirements for copper cavities having

---

[1] A Gaussian distribution does not significantly change the results.

Parameters	units	Type #1	Type #2
RF frequency	GHz	1.3	
Structure type		standing wave	
Dissipated power	MW	<4	
Aperture	mm	52	
Number of cells		5	17
Shunt impedance	MΩ/m	31.9	35.4
Accelerating gradient	MV/m	<14.8	<8.5
Length	m	0.576	1.96

Table 4.2.4: *Main characteristics of the accelerating structures for the bunching section.*

Parameters	units	results
Energy	MeV	11.3
Charge	nC	3.7
Phase extension (rms)	deg	5.3
Bunch length (rms)	mm	3.4
Energy spread (rms)	keV	45
Normalised emittance (rms)	mm mrad	42.5
Beam size σ_x	mm	2.6
Beam angular spread σ_{xp}	mrad	0.7

Table 4.2.5: *Summary of PARMELA simulations results at the buncher exit.*

high gradient and high average power also appear in the design of the positron pre-accelerator (PPA) (section 4.4), where new RF cavities (so-called CDS structures [34]) have been proposed. They have a high shunt impedance and can dissipate 30 kW/m. In addition they have a large iris aperture. The characteristics of the cavities used here are summarised in table 4.2.4.

The bunching section comprises two 5 cell cavities (type #1, see table 4.2.4), separated by a distance of $\lambda/2$ (115.3 mm) and sharing the power of one 10 MW klystron. The cavities are capable of producing up to 14.8 MV/m, but to provide a safety margin, simulations have been made using only 12 MV/m in each cavity.

In the simulations we assume for simplicity a 0.75 m long drift space between the source exit and the first prebuncher cavity, with one solenoidal lens in the middle. The lens is used to focus the beam into the first prebunching cavity.

The fields are optimised to achieve a minimum transverse emittance (figure 4.2.3). The magnetic field starts from about 50 Gauss after the first prebuncher, increases linearly to about 130 Gauss at the buncher entrance, where it then increases sharply to a value of 500 Gauss and stays constant over the length of the two buncher cavities. Steep transitions are necessary to fulfil the Brillouin conditions for laminar flow. The transitions are created using magnetically shielded solenoids. Simulation results obtained with PARMELA at the buncher exit, are summarised in table 4.2.5.
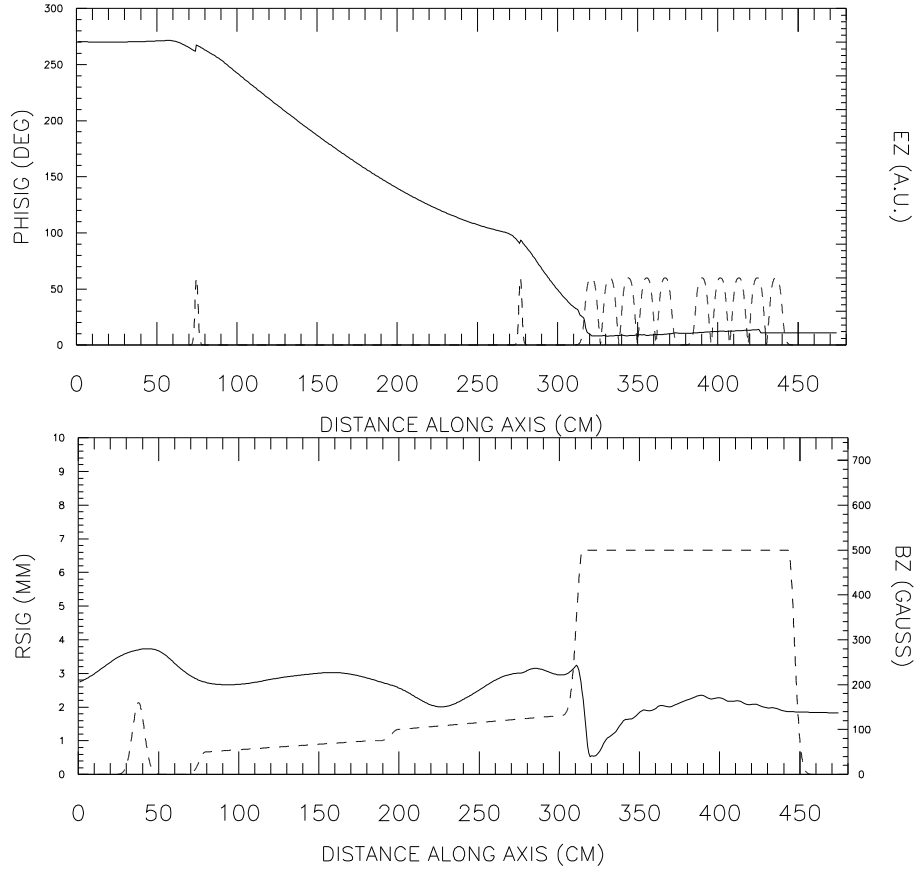
Figure 4.2.3:   *RMS beam radius and bunch length variation along the prebunching and bunching sections. The axial electric field (top) and the magnetic focusing field (bottom) are shown.*

Acceleration prior to injection into the SC linac

The choice of beam energy at the entrance of the first accelerator module of the injector linac is defined by the (non-normalised) beam emittance, which must be small enough to allow the beam to be easily transported through the module. As a goal, we have chosen the TTF injector normalised emittance of 20 mm·mrad for 8 nC bunches at 20 MeV, corresponding to a (un-normalised) emittance of 0.5 mm mrad at injection into the first cryomodule.

After the buncher, the beam energy is ~12 MeV. To provide the necessary acceleration, we will use the 17-cell cavities (table 4.2.4), which provide more energy than the 5-cell ones. One pair of cavities — powered with one standard 10 MW klystron — can give an energy gain of 32 MeV. Table 4.2.6 shows the expected beam emittance after one, two or three such units. One unit, resulting in a beam energy of 44 MeV, is sufficient to adiabatically damp the initial emittance to below the required 0.5 mm mrad (un-normalised): using two such pairs (76 MeV) provides a large and sufficient margin.

	E (MeV)	Norm. emittance	emittance
TTF injector	20	20.	0.5
proposed buncher	12	42.5	1.74
+ 1 klystron	44	42.5	0.49
+ 2 klystrons	76	42.5	0.28
+3 klystrons	108	42.5	0.20

Table 4.2.6: *Compared emittance (in mm mrad) of the TTF injector and of the proposed linac for beams of increasing energy.*

A spectrometer arm will be installed between the room temperature section and the SC linac so that the former can be independently operated and tuned. Two triplets are required for beam matching into the SC linac. A triplet is also necessary between the pairs of type #2 PPA cavities.

The 500 MeV superconducting linac

To achieve the required energy of 500 MeV, the SC linac has to provide 424 MeV to complement the 76 MeV from the room temperature section. Two standard linac cryomodules operated at a conservative gradient of 17.8 MV/m are used. One 10 MW standard klystron is sufficient to power both modules (see figure 4.2.1).

4.2.3   Electron source for the free electron laser (FEL)

The FEL source is treated in section 9.3. We mention it here only for completeness. It employs a 1-1/2 cell RF gun producing a 6.6 MeV beam which is subsequently injected into an accelerator module. The beam which exits the module at 155 MeV is slightly decelerated in a third harmonic (3.9 GHz) superconducting cavity which serves to correct the non-linear energy distribution of the beam. The FEL source also requires the use of a magnetic bunch compressor at an energy of 140 MeV as well as a further compressor at 500 MeV. To provide space for the compressors, only 3 modules are used in the FEL injector. The average gradient required in the last two modules is 25 MV/m. The 500 MeV bunch compressor will be based on the design used in the TTF linac.

4.2.4   The 5 GeV electron injector linac

The common injector linac accelerates the beam energy from 500 MeV to the damping ring energy of 5 GeV. It is a short version of the TESLA main linac and uses the same technology described in chapter 3. The energy gain of 4.5 GeV will be provided by 18×17 m modules (section 3.3) running at a gradient of $E_{acc} = 20$ MV/m and powered by six 10 MW klystrons. If one klystron fails, the linac can still be operated by increasing the gradient in the remaining sections (15 modules driven by 5 klystrons, corresponding to 24 MV/m).

For the FEL beam the injector linac is operated at lower gradient. We presently assume an FEL beam energy of $2.5\,\mathrm{GeV}$ at the injector linac exit (E_{acc}=8 MV/m), but there is a large flexibility to adjust this energy if desired.

The focusing is provided by a FODO structure with two accelerator modules per cell (one quadrupole in every module). The phase advance is 45° for the collider beam and up to about 100° per cell for the FEL beam.

4.3 Positron Source

A fundamental intensity limit for conventional positron sources is given by the thermal stress in the conversion target due to the energy deposition of the primary electron beam. For TESLA the target can be rotated within the long bunch train. With a target velocity of $50\,\mathrm{m/s}$ the heat load of about 100 bunches contributes to the thermal stress at a given position on the target. Table 4.3.1 compares the design parameters of TESLA with parameters reached at the SLC positron source, which has the highest intensity to date. The SLC source operates close to the stress limit of the target, and an extension of this technology by the required two orders of magnitude in intensity seems unrealistic. Therefore a new concept based on the conversion of high-energy undulator radiation in a thin target has been developed [22, 23]. The scheme also allows the possibility to produce polarised positrons; but since the technological demands for a polarised source are much higher than for an unpolarised source, only the latter will be considered for the initial TESLA run. The polarised source is considered as a possible upgrade to the machine at a later date.

parameter	SLC	TESLA
No. of positrons per pulse	$(3\text{–}5) \times 10^{10}$	5.6×10^{13}
No. of bunches per pulse	1	2820
pulse duration	$3\,\mathrm{ps}$	$0.95\,\mathrm{ms}$
bunch spacing	$8.3\,\mathrm{ms}$	$337\,\mathrm{ns}$
repetition frequency	$120\,\mathrm{Hz}$	$5\,\mathrm{Hz}$

Table 4.3.1: *Comparison of TESLA and SLC positron source parameters.*

4.3.1 General layout

A schematic of the source is shown in figure 4.3.1. The source is designed to produce twice as many positrons as required. In contrast to the original proposal in the CDR [6], the high-energy electron beam upstream of the interaction point (IP) is now used to generate high-energy photons in an undulator section positioned just downstream of the main linac. The original concept of using the spent electron beam (i.e. after collision) placed too many constraints on the design of the extraction line, and in particular suffered from unacceptably high distributed particle losses. Moving the e^+
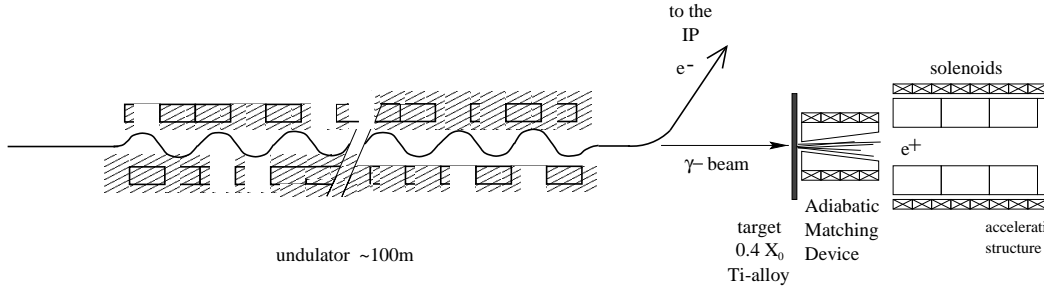
Figure 4.3.1: *Sketch of the positron source layout.*

source upstream of the IP has significantly simplified the extraction line and reduced the associated losses (see section 7.6). In addition, using the very high quality electron beam from the linac as opposed to the severely disrupted beam after the IP has increased the likelihood of realising a polarised positron source. The disadvantages of the location in front of the IP are that extra space and a positron transfer line to the other side of the interaction point (detector) are required. The undulator also slightly degrades the quality of the incoming electron beam, but the effects are considered acceptable.

The geometry of the source and the electron optics has been designed to accommodate the polarised source upgrade. For polarised positrons, the divergence of the high-energy photons from the helical undulator must be dominated by the $1/\gamma$ characteristic angle of the radiation, and only have a small contribution from the electron phase space. With the opening angle of the photons fixed by the electron beam energy, the beam size on the target is then only a function of distance. With a $250\,\mathrm{GeV}$ electron beam, corresponding to an angle of $1/\gamma \approx 2\,\mu$rad, a drift length to the target of $314\,\mathrm{m}$ is required to achieve the necessary target beam size of $0.7\,\mathrm{mm}$ (see section 4.3.7).

With the geometry and electron optics fixed by the polarised source, the unpolarised source requires a rather weak, long planar undulator $(K \leq 1)$[1] to keep the $0.7\,\mathrm{mm}$ beam size at the target. The photons are used to produce electron-positron pairs in the thin conversion target. The conversion of photons — rather than electrons as in a conventional source — leads to a small optimal target thickness of 0.4 of a radiation length (X_0). The conversion efficiency in a thin target depends only weakly on the target material: thus a low Z material such as titanium with a high specific heat capacity can be chosen. An additional advantage of the thin target is the smaller multiple-scattering which results in a higher capture efficiency. Both effects help to reduce the heat load on the target. The target has to rotate with a high velocity in order to withstand the long beam pulse.

The capture optics behind the target is of a conventional design. Since the positrons

---

[1]The K-value of an undulator is defined as: $K = eB\lambda_u/(2\pi m_e c)$, where B indicates the amplitude of the magnetic field and λ_u the undulator period. The K-value determines the spectral characteristics of the device and the opening angle of the radiation. For $K > 1$ the opening angle is K/γ.

have a broad distribution of transverse and longitudinal momenta, they must first be accelerated in RF cavities embedded in a solenoid field. The acceptance of a solenoid channel is characterised by a large transverse size and a small divergence, while the positrons emerging from the target have a small transverse size and a large divergence. To match the positrons to the acceptance of the solenoid, an adiabatic matching device (AMD) is used. It consists of a solenoid field which starts with a high initial field and tapers down adiabatically to the constant end field. After the AMD the positron beam will be captured and pre-accelerated to $\approx 250\,\text{MeV}$ in the normal conducting positron pre-accelerator (PPA). The beam is then transported through a transfer line under the detector hall, to the superconducting positron injector linac, where it is accelerated to $5\,\text{GeV}$ and injected into the damping ring (chapter 5).

The safety factor of two in the positron production rate is valid for $250\,\text{GeV}$ electron beam energy. When operating at a lower energy (i.e. lower centre of mass energy at the IP) this margin is reduced due to the strong dependence of positron production on photon energy. Without modifications, the source can be used down to about $160\,\text{GeV}$ (just below the top quark pair production threshold) without a significant intensity drop (the yield at this energy is ~ 1). In order to recover a high luminosity at even lower energy, e.g. at the Z^0 resonance, a scheme can be used in which the first part of the main linac ($\approx 50\,\text{GeV}$) accelerates the beam used for collisions, while the remainder ($\approx 200\,\text{GeV}$) accelerates the drive beam for the positron source. This option requires an additional drive beam injector and a $\sim 50\,\text{GeV}$ transfer line.

In the following sections, the various components of the positron source will be discussed in more detail.

4.3.2   Permanent magnet planar undulator

With a K-value of about 1 the spot size of the photon beam on the target is $0.7\,\text{mm}$, large enough to keep the thermal stress in the target low and small enough to obtain a high capture efficiency of the optics behind the target. The advantage of the planar undulator over the helical undulator required for the polarised positrons is the easier technology (permanent as opposed to superconducting magnets) and the accessibility from the side (important for field measurements, beam diagnostics pumping etc.).

The gap size of the undulator (in terms of nominal electron beam size) must be larger than the apertures defined by the downstream halo collimation system in the beam delivery system ($13\sigma_x \times 80\sigma_y$, section 7.5). Table 4.3.2 lists parameters of permanent magnet undulators with varying gap size and $K = 1$. With an elliptical vacuum chamber of half-gap $5\,\text{mm}\,(\text{h}) \times 1.5\,\text{mm}\,(\text{v})$, the (normalised) aperture is $79\sigma_x \times 350\sigma_y$, significantly larger than the collimation aperture.

With a vertical gap size of $5\,\text{mm}$ a field of $0.75\,\text{T}$ can be reached. The corresponding energy of the first harmonics is $28\,\text{MeV}$ and the required undulator length is $100\,\text{m}$ in this case. Note that due to the higher harmonics of the undulator radiation a significant amount of positrons are produced with an energy larger than $28\,\text{MeV}$.

gap [mm]	λ_u [cm]	B_{max} [T]	E_1 [MeV]
4.0	1.25	0.85	31.6
4.5	1.34	0.8	29.5
5.0	1.42	0.75	27.8

Table 4.3.2: *Parameters of the planar undulator.*

4.3.3   Influence of the undulator on the electron beam parameters

The main effect of the undulator on the electron beam is the mean energy loss of 1.2% (3 GeV) which has to be compensated by the main linac. The beam quality is deteriorated mainly in the longitudinal phase-plane by an increased energy spread of 0.15% as compared to 0.05% without the undulator [31].

The relative increase in horizontal transverse emittance from a perfect undulator is $\sim 3 \times 10^{-5}$ and can be ignored. Typical errors of the undulator magnets of $\Delta B/B = 1\%$, $\Delta\lambda_u/\lambda_u = 1\%$ and an rms rotation angle of 1 mrad lead to additional relative emittance contributions of $\sim 2 \times 10^{-3}$ and $\sim 1 \times 10^{-3}$ for the horizontal and vertical plane respectively [32].

4.3.4   Target

The positron production rate in the conversion target has been calculated with the code EGS4 [25] — a general purpose package for the Monte-Carlo simulation of electromagnetic showers. The optimum target thickness in terms of positron yield for a titanium alloy target is $0.4\,X_0$ (1.4 cm). The production rate in a titanium target is about 16% lower than in tungsten, but the higher heat capacity (by a factor of five) and the excellent mechanical properties of titanium allow much higher particle densities inside the target. The target has to rotate with a high velocity in order to avoid an overlapping of all bunches within one RF pulse. A velocity of about 50 m/s at the circumference of the target is necessary to spread out a single bunch train over a distance of 5 cm; this can be achieved with a target of 80 cm diameter rotating at 1210 revolutions per minute. The maximum heat load reached then corresponds to ~100 bunches overlapping at the same location, giving a temperature rise of about 420°C. The diameter is chosen to evenly distribute the heat load over the entire circumference of the target over many 5 Hz pulses. The average heat load amounts to 5 kW. Cooling by radiation might be sufficient in the case of the large target wheel, but this needs further investigation. Cooling with water is possible with a vacuum feed-through based on a design from CERN [28], which uses differential pumping.

4.3.5   The adiabatic matching device (AMD)

The particles which emerge from the target have to be accelerated in a cavity embedded in a solenoid field for focusing: it is here that the final emittance and the efficiency of the positron source are defined. Because the multiple-scattering is reduced in a thin

target (compared to the thick target of conventional sources), the transverse momenta of the positrons emerging from the target are smaller, resulting in a higher capture efficiency. In order to match the phase space of the positron beam (characterized by a small spot size and a large divergence) to the acceptance of the solenoid (large spot size and a small divergence), a matching section is introduced between the converter target and the first accelerating cavity. The matching section consists of a so-called adiabatic matching device (AMD), a tapered solenoid starting with a high initial field and tapered adiabatically down to the constant end field. The acceptance of the system is matched to the acceptance of the damping ring so that no further particle losses occur in the ring itself.

Two mechanisms lead to an emittance growth of the positron beam in the matching device and hence to additional particle losses:

- emittance growth due to non-adiabatic fields; and

- bunch lengthening due to path length and velocity differences.

A solution for the particle motion in an adiabatically varying solenoid field has been found [29], from which the optimum on-axis field distribution for the matching device along the longitudinal coordinate z is given by:

$$B(z) = \frac{B_i}{1 + g \cdot z},$$

where B_i is the initial solenoid field and g the taper parameter. The condition for an adiabatic field variation is then given by $(gP)/(eB_i) \ll 1$ ($P=$ particle momentum). In order to fulfil this condition for particles with higher energy the taper parameter g has to be small: however, this means that the matching section becomes long, and the bunch lengthening becomes stronger. An optimum is reached with $g = 30\,\mathrm{m}^{-1}$ in the present design. An overall capture efficiency of 16% can be reached with an initial field of 6 T. Fields of up to 8 T have already be realised [30] and 10 T seems feasible: however, since the bunch train is long the production of a higher field with a pulsed device is more difficult, and a lower field seems to be more reasonable.

Table 4.3.3 lists the important parameters of the positron source.

4.3.6   Low intensity auxiliary source

For the commissioning of the various positron accelerator systems, a source which works independent of the main electron linac is desirable. An electron beam of 500 MeV is sufficient to produce a few per cent of the design positron current using the same thin titanium target and the capture optics of the high intensity source. The heat load on the target is high, but does not reach the limits discussed in [23]. The electron source is a copy of the main electron injector (see section 4.2).

It is foreseen to use the same gun as the (second) electron source when TESLA is operated as a $\gamma\gamma$ or e^-e^- collider. It should be noted that in these cases, a polarised electron source is required.

Undulator	
peak field	0.75 T
period length	14.2 mm
gap height	5 mm
γ-spot size on target	0.7 mm
photon beam power	135 kW
Target	
material	Ti-alloy
thickness	1.42 cm $(0.4X_0)$
pulse temperature rise	420 K
av. power deposition	5 kW
Adiabatic Matching Device	
initial field	6 T
taper parameter	$30\,\mathrm{m}^{-1}$
end field	0.16 T
capture cavity iris radius	23 mm
General	
capture efficiency	16%
No. of positrons per electron	2
norm. e^+-beam emittance	0.01 m
total energy width	±30 MeV
required D.R. acceptance	0.048 m

Table 4.3.3: *Overview of the positron source main parameters.*

4.3.7   Potential upgrade to a polarised positron source

The proposed positron source opens up the possibility to produce polarised positrons: circularly polarised photons produced by high-energy electrons in a helical undulator convert to polarised e^+e^- pairs in the target [22, 23]. However, the technological challenges of a polarised source are far more demanding than for the unpolarised source, and the polarised source is considered as a potential future upgrade.

In order to produce circularly polarised photons, a short period helical undulator of about 100 m length has to be used instead of the planar wiggler. Since only the on-axis photons are completely circularly polarised, off-axis photons have to be collimated; this requires that the photon beam spot size at the target is dominated by the natural opening angle of the radiation ($\sim 1/\gamma$). The distance between the undulator and the target has to be large (>150 m) to achieve the required target photon beam size (0.7 mm), and the electron beam divergence in the undulator has to be small compared to $1/\gamma$. The parameters of the helical undulator are demanding and have so far not been demonstrated. With a period length of 1 cm an on-axis field of 1.3 T has to be reached. The parameters can currently only be realised with superconducting technology at a gap radius of about 2 mm [33]. A detailed design of such an undulator with the required parameters is still to be done.

The collimation of a large fraction of the photons — necessary to increase the degree of polarisation — requires the development of high-power collimators. The average power deposition in the collimators can reach several $100\,\text{kW}$. The polarisation of the circularly polarised photons is transferred to the electron-positron pairs during pair production. For the calculation of the processes in the target the EGS4 code has been extended [23]. The code includes polarisation effects for pair production, bremsstrahlung and Compton scattering. Simulation results indicate a maximum longitudinal positron polarisation of 45–60%.

4.4 Positron Injection System

The positron injection system consists of three sections:

- a normal conducting pre-accelerator which captures the positrons, separates them from the electrons and the photon beam, and accelerates them up to an energy of $250\,\text{MeV}$;

- a long transfer line which guides the positrons below the experimental hall to the other side of the IP;

- a superconducting accelerator to bring the positrons to the damping ring energy of $5\,\text{GeV}$.

The layout and the main results of the optimisation of the complete positron injection system are presented below. For further scientific and technical details of the design we refer to the detailed reports [34, 35].

4.4.1 Positron pre-accelerator (PPA)

The purpose of the PPA is to provide a maximum capture efficiency for that part of the emerging positron beam which is within the damping ring acceptance; this 'useful' part of the beam has an energy spread $\Delta E/E_f = \pm 6\%$ for the PPA output energy of $250\,\text{MeV}$ and a phase spread $\Delta\varphi = \pm 7.5^o$ with respect to the PPA RF-frequency of $1.3\,\text{GHz}$. The total normalised transverse e^+ beam emittance is limited by $\varepsilon_x < 0.036\text{m}$, $\varepsilon_y < 0.036\text{m}$, and $\varepsilon_x + \varepsilon_y < 0.048\,\text{m}$ for the PPA and other parts of the injector. The capture efficiency is defined as the ratio of the number of positrons inside this acceptance to the total number of positrons escaping from the target.

The general layout of the PPA is shown in figure 4.4.1. The PPA is a standing-wave normal-conducting linac. The front end of the PPA consists of acceleration cavities embedded in a focusing solenoid. The first two cavities (figure 4.4.2) have a high accelerating gradient ($E_{acc} = 14.5\,\text{MV/m}$), to reduce bunch lengthening, whereas the others have moderate gradients ($E_{acc} = 8.5\,\text{MV/m}$) to reduce RF power consumption. Each cavity is powered by one standard TESLA $10\,\text{MW}$ klystron through a single RF coupler (figure 4.4.2). An additional bunch length reduction is achieved by inserting the first cavity into the AMD by $\approx 60\,\text{cm}$.
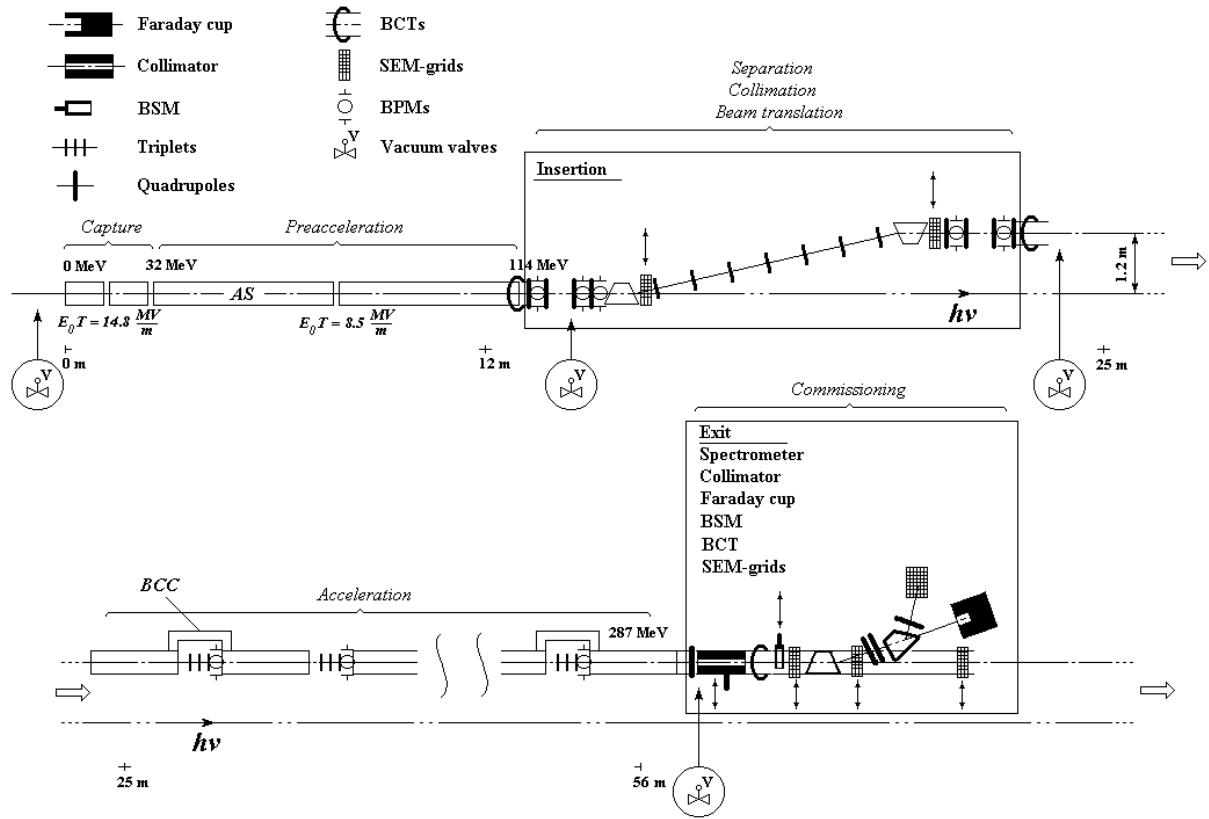
Figure 4.4.1: *Conceptual layout of the PPA.*

With the long RF pulse (950μs flat-top) and repetition rate of 5 Hz, the achievable gradients in the first and second cavity of the PPA are limited by RF power and heat load restrictions. Three dimensional thermal stress analysis indicates that stable and reliable cavity operation with a heat load of about $30\,$kW/m is possible, corresponding to an accelerating gradient $E_{acc} = 14.5\,$MV/m [34, 36].

About 65% of the incoming positrons and 76% of the incoming electrons will be lost in the AMD and the first four cavities, resulting in an enhanced radiation level and additional heating.

Located downstream of the PPA (at a positron beam energy of 114 MeV) is a magnetic insertion to separate the positrons and the remaining electrons. The insertion makes a parallel translation of the PPA axis by a distance of 1.2 m; this provides a sufficient clearance for the photon beam and allows collimation of the positron beam. The insertion has a standard achromatic design with two bend dipoles and matching sections at both ends (figure 4.4.3). Non-linear chromatic effects are the dominant factors for the final beam quality when transporting the low energy beam with high relative energy spread [35]. The total positron losses in the separator (composed mainly of particles with a large momentum deviation) are estimated at $\sim$8.4 % of the incoming
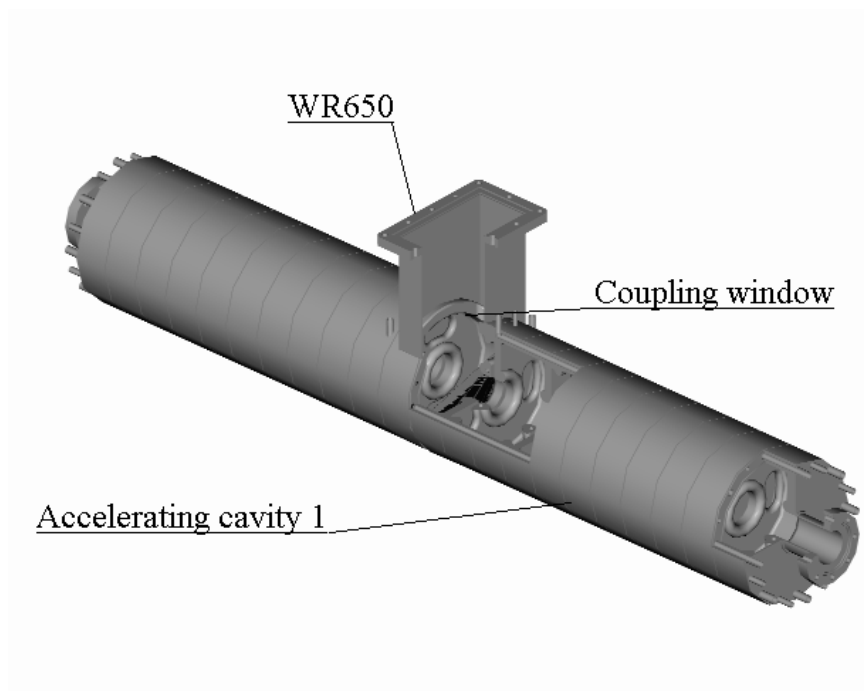
Figure 4.4.2: *Short accelerating cavity for the first part of the PPA.*
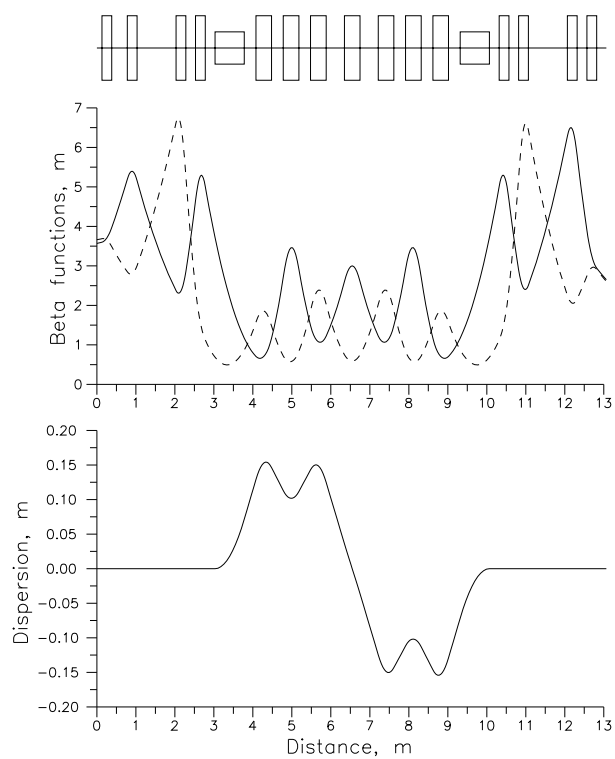
Figure 4.4.3: *Optical functions in the separator section.*
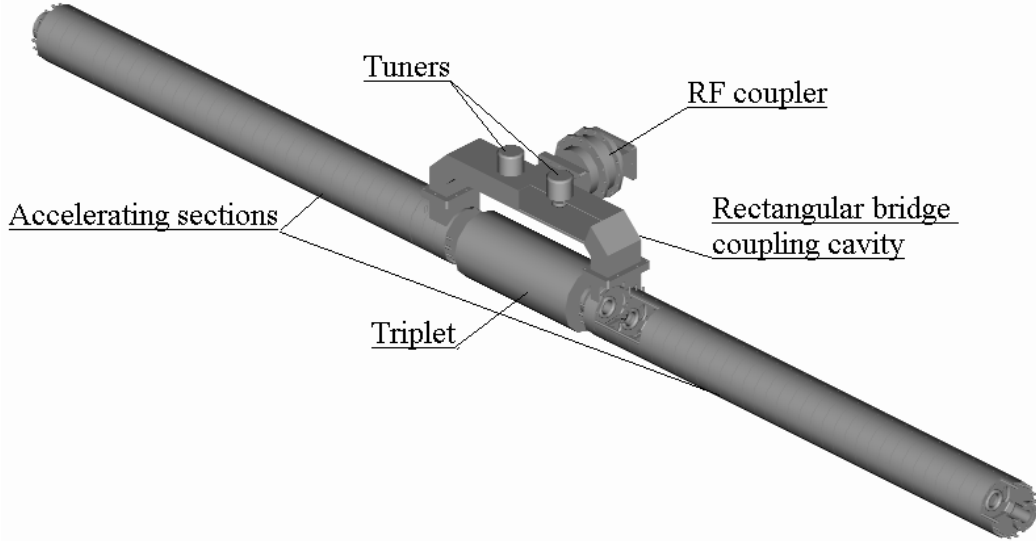
Figure 4.4.4: *Accelerating cavity in the downstream part of the PPA.*

e^+ beam. Behind the first dipole of the separator there is a dump system, which can handle the residual e^- beam up to an average power of 12–15 kW.

After the separator the positron beam has practically a single-bucket structure (the first e^+ bunch has $\sim 99.3\%$ of the total number of positrons); the population of neighbouring RF-buckets present before the insertion [34] has practically vanished. The downstream part of the PPA consists of five cavities with moderate gradient (8.5 MV/m). Each cavity has two accelerating sections (figure 4.4.4). The transverse focusing is accomplished using quadrupole triplets, placed between the sections, which are separated by a drift space of $4\lambda_{RF}$. To combine two sections into a single resonant system, bridge coupling cavities are used. Each cavity is powered by one 10 MW klystron. The phase space distribution at the PPA exit is shown in figure 4.4.5.

The main PPA parameters are listed in table 4.4.1. The total PPA length is 55 m and the transverse dimensions are small enough to allow clearance to the neighbouring magnets of the high-energy electron switch-yard and beam delivery system (see chapter 7). The nine klystron stations (plus one spare for fast exchange in case of a failure) will be placed in the second-IR switch-yard shaft which also houses the positron target.

The coils of all magnetic elements placed in areas with large particle losses (the solenoid in the first part of the PPA, quadrupoles and bending magnets in the PPA insertion) have to be made from a special cable with mineral insulation.

Due to the strong non-linear effects in the magnetic insertion, this area is equipped
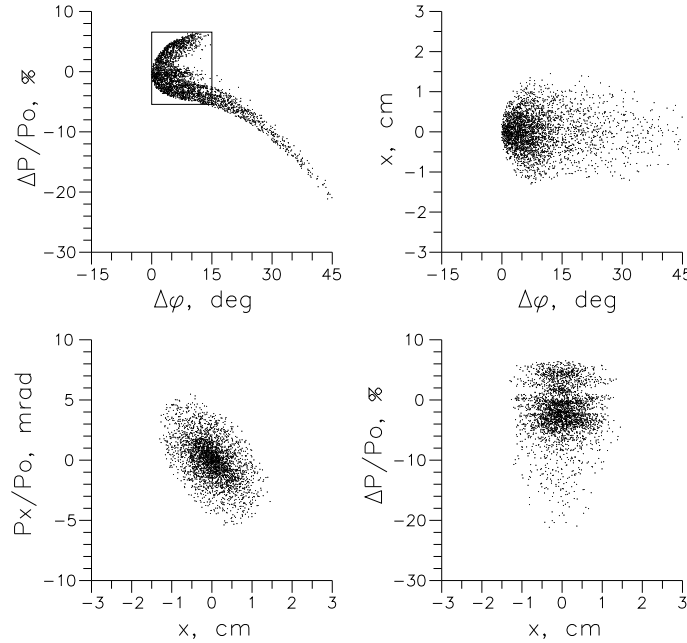
Figure 4.4.5: *Positrons phase space plots at the PPA exit.*

Parameter	value
Final energy E_f, MeV	287
Total capture efficiency, %	21.3
Solenoid length, m	~11.4
Solenoid field, T	0.22
Number of quadrupoles	42
Number of dipoles	2
Number of klystrons	9
Total length, m	~55.5

Table 4.4.1:   *The main parameters of the PPA.*

with instrumentation to verify the beam parameters. All quadrupoles have integrated position monitors. In addition, two secondary emission (SEM) grid monitors are foreseen behind the bending magnets for beam profile measurements. A complete set of beam monitors is foreseen at the PPA exit, mainly for linac commissioning. The PPA subsystems are described in detail in [34] and [35].

4.4.2   Shielding requirements for the target and PPA area

Since the energy of the undulator photons is below the muon production threshold of 210 MeV, no muons will be produced in the target. Therefore the major radiation source during operation is the photon induced neutron production in the target,

adiabatic matching device, and the first section of the accelerator. To protect the surrounding environment from the high neutron flux, these components will be embedded in a concrete cave of up to $1.5\,$m wall thickness. The embedded section will be assembled on a common girder and all connections (power cables, cooling water etc.) will be outside of the cave. The shielding requirements for the downstream sections are more relaxed and can be realised with concrete blocks (in the separation and collimation section) or lead walls. The induced activity after 5000 hours of operation can be shielded with lead of $\leq 15\,$cm thickness even in the target area. In case of a failure it is foreseen to exchange complete sections (girders) rather than single components.

4.4.3   Low-energy transfer line

The general layout of the transfer line is shown in figure 4.4.6. The line must:

- use the existing TESLA tunnel (with the exception of the bypass section);

- provide a vertical bypass section between the two main dump halls, that passes under the detector hall;

- provide adjustable matching to the beam parameters at the PPA exit and superconducting accelerator entrance;

- not introduce dispersion (except in the bypass section);

- keep the bunch length constant.
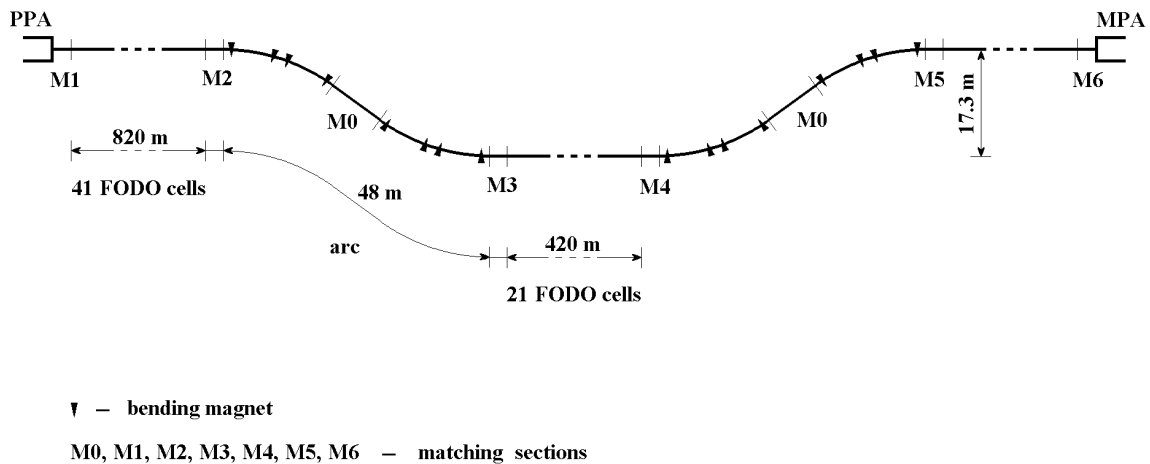
Figure 4.4.6: *Schematic layout of the low-energy transfer line.*
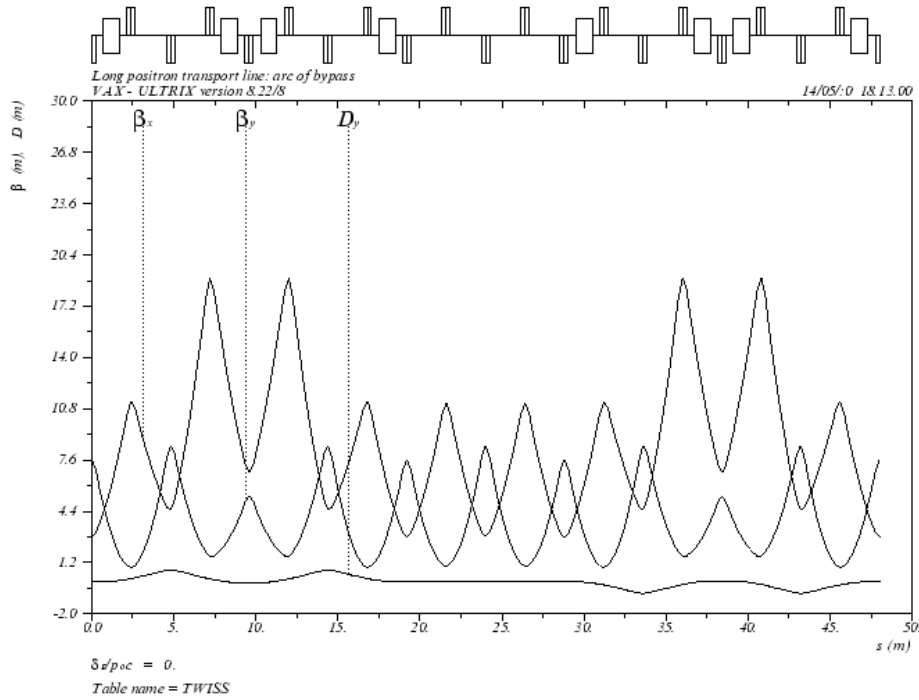
Figure 4.4.7: *Optical functions along one bypass arc.*

There are a few special aspects which complicate the design of the transport system:

- the transfer line is long, and therefore the aperture versus the number of magnets needs to be optimised; and

- it must transport a beam with large transverse emittance and a large energy spread, resulting in large magnet apertures and a quasi-isochronous bypass design.

For the long straight sections a FODO type structure is used. The parameters of the FODO cell have been optimised with respect to the maximum beam size, maximum tolerable modulation of the β-function, and the number of quadrupoles in the line.

As a result of various studies the following scheme has been chosen for the bypass. Each arc of the bypass section consists of two quasi-isochronous cells connected by a matching section (figure 4.4.7). It is convenient to construct the matching section from the same FODO cells (without bending magnets) used in the isochronous cells. Two quasi-isochronous cells plus two FODO matching cells are sufficient to reach a (downward) vertical displacement of 17.3 m. The quasi-isochronous cells of the bypass are based on a modified four-cell FODO structure with missing magnets. The longitudinal dispersion (R_{56}) of the bypass and hence of the complete transfer line is tunable and can be used to further compress the bunch.

Parameter	Value	Unit
Kinetic energy	287	MeV
Total length	2208.3	m
Length of bypass arc	48	m
Translation base	17.3	m
Normalised emittances		
horiz.	0.036	m
vert.	0.036	m
Energy spread	±0.06	
Number of quadrupoles	276	
Number of dipoles	16	

Table 4.4.2:   *Main parameters of the low-energy positron transfer line.*

The main parameters of the transfer line are summarised in table 4.4.2. All quadrupoles have the same dimensions, differing only in the gradient G_0, and can be divided in two groups: those with low gradient $G_0 \leq 0.3\,\text{T/m}$, (211 units); and those with moderate gradient $0.3\,\text{T/m} \leq G_0 \leq 1.5\,\text{T/m}$ (65 units). The DC power required for one low gradient FODO quadrupole is 60 W. The lenses can be made without water cooling to reduce costs. The aperture diameter for all quadrupole lenses is equal to 0.16 m, providing a 1.7 safety factor with respect to the full size of the beam for the FODO cells and more than a factor of two for all matching and bypass quadrupoles (except for four quadrupoles in each bypass arc). This choice is a reasonable compromise between the safety factor and the number of magnetic elements. Other details of the transfer line design are described in [35].

4.4.4   Superconducting positron injector linac (PIL)

The general layout of the positron injector linac is shown in figure 4.4.8. The linac is based on the standard TESLA nine-cell superconducting accelerating structure. Due to the large transverse emittances of the e^+ beam the transverse focusing in the linac is based on superconducting quadrupole doublets. The safety factor, calculated as a ratio of the inner radius of an element to the maximum beam envelope in that element, is >2. Two types of cryomodules[1] are assumed in the design: the first type (CM-1) contains four accelerating structures and four doublets, while the second one (CM-2) consists of eight structures and a single doublet [35]. The design of the doublets is based on the main linac quadrupole. It is possible to keep the gradient to $\sim 60\,\text{T/m}$ with an effective length of $\sim 200\,\text{mm}$ for each quadrupole in the CM-2 modules: thus these doublets have the same length as the standard linac quadrupole. The doublets for the CM-1 type modules are longer and replace every second accelerating cavity. Eight

---

[1]The design of the positron pre-accelerator has been based on TTF-like 12 m long modules. It is also conceivable to use the standard 17 m long modules as in the main linac, thus avoiding building two types of modules of different length.
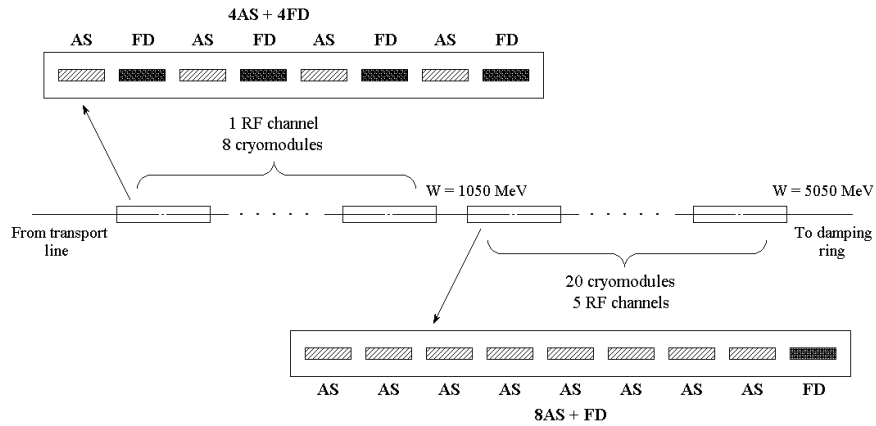
Figure 4.4.8: *Conceptual layout of the sc positron injector linac (AS = accelerating struc-ture, FD = quadrupole doublet).*
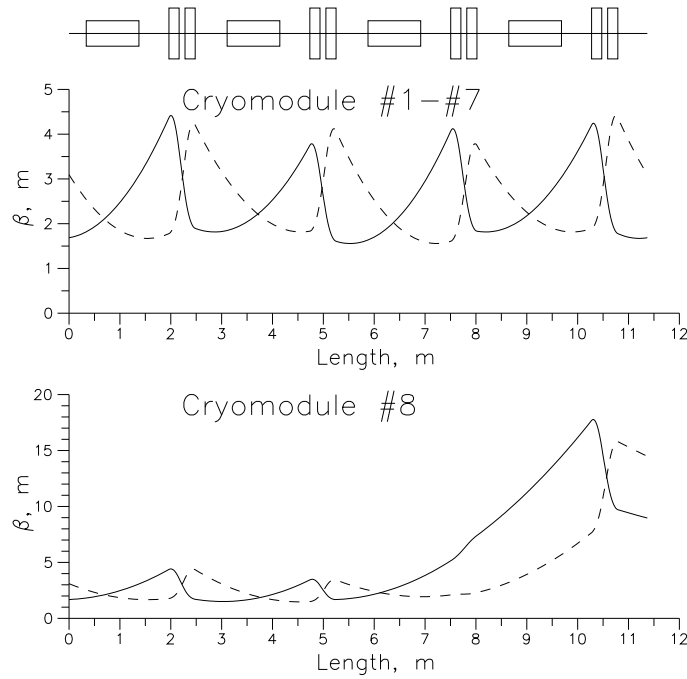
Figure 4.4.9: *β-functions for the eight CM-1 modules.*

CM-1 type modules are used in the first part of the injector linac (up to a positron energy of $\approx 1\,\mathrm{GeV}$). The eighth module is used as a matching module (figure 4.4.9). The remainder of the linac (up to $5\,\mathrm{GeV}$) is constructed from 20 CM-2 modules. The standard TESLA RF distribution scheme and hardware are used.

The general parameters of the injector linac are listed in table 4.4.3. More details
of the injector linac design can be found in ref [35].

Cryomodule CM-1	
Number of cryomodules	8
Cryomodule length [m]	11.368
Energy gain per cryomodule [MeV]	100
Number of quadrupole doublets	4
Number of accelerating sections	4
Cryomodule CM-2	
Number of cryomodules	20
Cryomodule length [m]	12.352
Energy gain per cryomodule [MeV]	200
Number of quadrupole doublets	1
Number of accelerating sections	8
Final beam energy [GeV]	~ 5.08
Total length [m]	~ 338
Safety factor	> 2
Total number of klystrons	6
Total number of cryomodules	28
Total number of quadrupole doublets	52
Total number of accelerating sections	192

Table 4.4.3:   *The main parameters of the positron injector linac.*

4.4.5   Summary of the positron injector

In this final section we briefly summarise the major points of the positron production
system. Details can be found in the preceding sections.

The positron injector consists of several essentially different parts: a normal con-
ducting positron pre-accelerator (PPA); a low-energy transport line (including bypass
sections); and a superconducting injector linac. The parameters for each sub-system
are optimised to obtain an effective, technically realisable and cost-effective solution.

The PPA is a standing-wave normal-conducting linac; its design is based on ex-
perience from existing linear accelerators and standard TESLA RF equipment. The
low-energy transfer line magnets have conservative cost-effective parameters. The sc
injector linac is based on standard TESLA/TTF equipment.

The total positron transmission of the injector from the target to the exit of the
pre-accelerator is estimated at $\approx 16\%$. This value is sufficient to provide the necessary
positron intensity for the 500 GeV collider with a safety

Bibliography

[1] S. Schreiber et al. , *Performance Status of the RF-Gun Based Injector of the TESLA Test Facility Linac*, Proc. 7th EPAC, Vienna 2000, p. 309.

[2] B. E. Carlsten, *New Photoelectric Injector Design for the Los Alamos National Laboratory XUV Fel Accelerator*, Nucl. Instr. Meth. **A285** (1985) 313.

[3] P. Michelato, C. Pagani, D. Sertore, A. di Bona, S. Valeri, *Characterization of Cs_2Te photoemissive film: Formation, spectral responses and pollution*, Nucl. Instr. Meth. **A 393** (1997) 464.

[4] P. Michelato et al., *High Quantum Efficiency Photocathode Preparation System for TTF Injector II*, Proceedings of the 21st International FEL Conference, Hamburg 1999, Vol. II, p.97.

[5] R. Brinkmann et al., *A Flat Beam Electron Source for Linear Colliders*, DESY TESLA-99-09, 1999.

[6] R. Brinkmann et al. (Eds.), *Conceptual Design of a 500 GeV e^+e^- Linear Collider with Integrated X-ray Laser Facility*, Vol. I, DESY report 1997-048 and ECFA 1997-182, 1997.

[7] R. Alley et al., *The Stanford Linear Accelerator Polarised Electron Source*, Nucl. Inst. and Meth. **A 365**, p.1 (1995)

[8] The NLC Design Group, *Zeroth-Order Design Report for the Next Linear Collider*, SLAC Report 474, pp 28-34 (1996)

[9] M. Breidenbach et al., *An Inverted-geometry, High Voltage Polarized Electron Gun with UHV Load Lock*, Nucl. Instrum. And Meth. **A 340** (1994)

[10] M. Woods et al., *Observation of a Charge limit for Semiconductor Photocathodes*, J. Appl. Phys. **73** 8531 (1993)

[11] W. E. Spicer and A. Herrera-Gomez, *Modern Theory and Applications of Photocathodes*, SLAC-PUB-6306 and Proc. SPIE 2022 51 (1993)

[12] D. Schultz et al., *The Polarized Electron Source of the Stanford Linear Accelerator Center*, SLAC-PUB-6606, August 1994; presented at 17th International Linear Accelerator Conference (LINAC 94), Tsukuba, Japan, 21-26 Aug (1994)

[13] J. E. Clendenin, *Polarized Electron Sources*, SLAC-PUB-95-6842, May 1995 and Proc. of Particle Accelerator Conference PAC 95, Dallas, Texas, 1-5 May 1995, pp 877-881 (1995)

[14] F. Stephan et al., *Photo Injector Test Facility under Construction at DESY Zeuthen*, Proc. Free Electron Laser Conf., 13-18 Aug. 2000, Durham, North Carolina.

[15] W. Koechner, *Solid-State Laser Engineering*, Berlin 1999, p. 406.

[16] White et al., *120-fs Terawatt $Ti:Al_2O_3/Cr:LiSrAlF_6$ Laser System*, Opt. Lett. 17 1067 (1992);
Ditmire, Perry, *Terawatt $Cr:LiSrAlF_6$ Laser System*, Opt. Lett. **18** (1993) 426.

[17] I. Will, P. Nickles, W. Sandner, *A Laser System for the TESLA Photo-Injector*, Internal Design Study, Max-Born-Institut, Berlin, 1994.

[18] *Running Experience with the Laser System for the RF Gun based Injector at the TESLA Test Facility Linac*, Nucl. Instrum. Meth. **A445** (2000) 427.

[19] A. Curtoni, M. Jablonka, *Study of the TESLA preaccelerator for the polarized electron beam*, DESY TESLA-01-22, 2001.

[20] R. Brinkman et al. (Eds.), ,*Conceptual Design Report of a 500 GeV e^+e^- Linear Collider*, Vol. II, DESY 1997-048, p. 697-726.

[21] D. A. Edwards (Eds.), ,*TESLA TEST FACILITY design report*, DESY TESLA-95-01, 1995, p. 57-92.

[22] V. E. Balakin and A .A. Mikhailichenko, *The Conversion System for Obtaining High Polarized Electrons and Positrons*, Preprint INP 79-85, 1979.

[23] K. Flöttmann, *Investigations Toward the Development of Polarized and Unpolarized High Intensity Positron Sources for Linear Colliders*, DESY-93-161, 1993.

[24] R. Brinkmann, J. Pflüger, V. Shiltsev, N. Vinokuro, P. Vobly, *Wiggler Options for TESLA Damping Ring*, DESY-TESLA-95-24, 1995.

[25] W. Nelson, H. Hirayama and D. Rogers, *The EGS4 Code System*, SLAC-265, 1985.

[26] S. Ecklund, *Positron Target Materials Tests*, SLAC Collider Note-128, 1981.

[27] E. M. Reuter and J. A. Hodgson, *3D Numerical Thermal Stress Analysis of the High Power Target for the SLC Positron Source*, SLAC-PUB-5370, 1991.

[28] P. Sievers and M. Höfert, *A Megawatt Electron Positron Conversion Target — A Conceptual Design*, Proc. 1st EPAC, Rome 1988.

[29] R. H. Helm, *Adiabatic Approximation for Dynamics of a Particle in the Field of a Tapered Solenoid*, SLAC-4, 1962.

[30] H. Ida, *Present R&D Status of Positron Sources for JLC-1 and ATF*, presented at 6th International Workshop on Linear Colliders, Tsukuba 1995.

[31] E. L. Saldin, E. A. Schneidmiller, M. V. Yurkov, *Calculation of Energy Diffusion in an Electron Beam due to Quantum Fluctuations of Undulator Radiation*, DESY TESLA-FEL 96-05, 1996.

[32] R. Glantz, *A Feasibility Study of High Intensity Positron Sources for the S-Band and TESLA Linear Colliders*, DESY-97-201, 1997.

[33] K. Flöttmann, S. Wipf, *Field Enhancement of a Superconducting Helical Undulator with Iron*, DESY TESLA-96-05, 1996.

[34] K. Flöttmann, V. Paramonov ed., *Conceptual design of a Positron Pre-Accelerator for the TESLA Linear Collider*, DESY TESLA-99-14, 1999.

[35] K. Flöttmann, V. Paramonov ed., *Conceptual Design of a Positron Injector for the TESLA Linear Collider*, DESY TESLA-00-12, 2000.

[36] V. Paramonov, I. Gonin, *3D Thermal Stress Analysis for the CDS Structure*, Proc. 7th EPAC, Vienna 2000, p. 1990.